J Therm Anal Calorim (2011) 103:1001–1006
DOI 10.1007/s10973-010-1135-8

DSC analysis of isothermally melt-crystallized bacterial poly(3-hydroxybutyrate-*co*-3-hydroxyhexanoate) films

Changkun Ding · Bowen Cheng · Qiong Wu

Received: 23 July 2010 / Accepted: 26 October 2010 / Published online: 8 December 2010

Abstract The multiple melting behavior of isothermally melt-crystallized poly(3-hydroxybutyrate-*co*-3-hydroxyhexanoate) (PHBHHx) from its melt was investigated using differential scanning calorimetry (DSC). PHBHHx exhibits a fourfold endothermic melting phenomenon, which were expressed as A, I, II, and III from low to high temperature, and attributed to the melting of secondary lamellae formed at room temperature, the melting of secondary lamellae at crystallization temperature, the melting of primary lamellae, and the melting of the recrystallized lamellae of different stabilities, respectively. Secondary crystallization is much slower than the primary crystallization and needs a relatively long period of time to occur. Furthermore, secondary crystallization at room temperature is heterogeneous, which depends on the presence of the primary lamellae and the secondary lamellae formation.

Keywords PHBHHx · Multiple melting behavior · Primary and secondary crystallization · Differential scanning calorimeter · Endotherm

C. Ding · B. Cheng (✉)
School of Materials Science and Engineering, Tianjin Polytechnic University, Tianjin 300160, People's Republic of China
e-mail: bowen15@tjpu.edu.cn

Q. Wu (✉)
Department of Biological Science and Biotechnology, Tsinghua University, Beijing 100084, People's Republic of China
e-mail: wuqiong@mail.tsinghua.edu.cn

Introduction

Polyhydroxyalkanoates (PHA) are intracellular biopolyesters which are accumulated by a number of bacteria as carbon and energy storage materials. These microbial PHA polymers have received a lot of attention as environmentally friendly thermoplastics for environmental, agricultural, medical, and tissue engineering applications [1–3]. Poly(3-hydroxybutyrate-*co*-3-hydroxyhexanoate) (PHBHHx), a new member of PHA family has been biologically synthesized [4–7] and produced on a large scale [8]. The mechanical and process properties of PHBHHx are better than those of poly(3-hydroxybutyrate) (PHB) and poly (3-hydroxybutyrate-*co*-3-hydroxyvalerate) (PHBV) [4]. Compared with poly(L-lactide) (PLLA) and PHB, PHBH Hx also has a better biocompatibility with chondrocyte [9–12], fibroblast [13–15], osteoblast [15, 16], smooth muscle cells [17–19], and nerve cells [20].

Thermal analysis is a powerful tool for characterizing the physical–chemical properties of biodegradable polymers [21–24]. Isothermally crystallized semicrystalline polymers often exhibit a multiple melting behavior, which is a key subject for investigating the structure evolution of polymers during the heating process. In recent years, a large amount of studies have been performed on the multiple melting behavior of some polymers, e.g., poly(butylene succinate) (PBS) [25–28], PLLA [29, 30], PHB [31], and PHBV [32, 33]. Attempts were made to explore the origin of the multiple melting behavior in some semicrystalline polymers. The behavior may result from [34]: (a) the presence of more than one crystal modification, (b) variation in morphology (such as lamellar thickness, distribution, perfection or stability), (c) melting–recrystallization–remelting mechanism during the DSC heating process, (d) physical aging or/and relaxation of the rigid

amorphous fraction, (e) different molecular weight species, and (f) orientation effects and so forth.

However, in terms of the multiple melting behavior of PHBHHx, only few work have been reported [5, 35–43]. In this work, the multiple melting behavior of isothermally melt-crystallized PHBHHx films was studied using the conventional differential scanning calorimetry (DSC) technique. Unusual fourfold melting endotherms were observed. A new and comprehensive explanation on the origin of the complex multiple melting behavior particularly the origin of the secondary crystallization, which is different from previous work, will be given in detail.

Experimental

Materials

PHBHHx was biosynthesized at Tsinghua University in Beijing, China, with the bacterial strain *Aeromonas hydrophila* 4AK4 in a glucose mineral-salt medium [7]. The weight-average molecular weight (M_w), number-average molecular weight (M_n), and M_w/M_n (PDI) for PHBHHx sample were determined by gel permeation chromatography (Shimadzu, Lc-20A) to be 2.59×10^5, 1.19×10^5, and 2.18, respectively. The molar ratio of 3HB/3HHx was determined to be 85/15 by ^{1}H-NMR (Bruker, Avance Av). Before use, PHBHHx was purified by dissolving it in chloroform, precipitating in ethanol, and then vacuum dried at 60 °C for 48 h. Chloroform and ethanol were purchased from Kermel Chemical Reagent Development Center, Tianjin, China.

Sample preparation

All PHBHHx films of 50 μm thickness were initially prepared by conventional solvent-cast techniques from chloroform solutions of PHBHHx using Teflon sheets as casting surfaces. The resulting films were further dried in vacuum at 60 °C for 24 h to remove any residual solvent and moisture. Films were stored in desiccator under nitrogen atmosphere prior to use. Then, these PHBHHx films were melted at 150 °C for 3 min and rapidly transferred onto a hot-stage (JYL/KWL 300, Beijing Jieyali Electronics and Technology Co. Ltd, China) preset at a given crystallization temperature (T_c) and isothermally crystallized at T_c for 2 days. The melt-crystallized samples were stored at room temperature for at least 2 weeks before further analytical measurements.

Differential scanning calorimetry measurements

DSC data of melt-crystallized PHBHHx samples were measured between 20 and 150 °C with a NETZSCH DSC 200 F3 (NETZSCH Co., Germany) under nitrogen (30 mL min^{-1}) and using a heat rate of 10 °C min^{-1} for most tests. Other heating rates used will be discussed in the specific section. A fresh sample was used in each run.

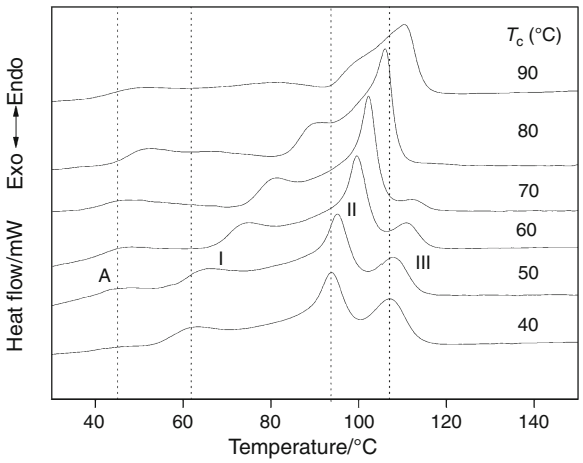

Fig. 1 Subsequent melting curves of PHBHHx samples isothermally melt-crystallized at different T_c for 2 days and stored at room temperature for at least 2 weeks (heating rate 10 °C min^{-1})

Results and discussion

Multiple melting behavior of isothermally melt-crystallized PHBHHx films

Figure 1 shows subsequent melting endotherms (10 °C min^{-1}) of PHBHHx solvent-cast films, which were isothermally melt-crystallized for 2 days at various T_c (40–90 °C) and stored at room temperature for at least 2 weeks. As shown in Fig. 1, fourfold melting endotherms (A, I, II, and III) were observed with peak melting temperatures T_m(A), T_m(I), T_m(II), and T_m(III) according to the order of their positions, respectively.

From Fig. 1, the multiple melting behavior of PHBHHx is obviously dependent on T_c. Both T_m(I) and T_m(II) shifted toward higher temperature with increasing T_c. The magnitudes of endotherm II increased and the shape became sharper and narrower as T_c increased, while those of endotherm I increased slightly with increasing T_c. In addition, endotherm III decreased gradually and disappeared when T_c is up to 90 °C. At high temperature (90 °C), endotherms I and II merged and appeared as a weak shoulder. These results suggested that endotherm II probably corresponds to the melting of primary lamellae and endotherm I is associated with the melting of secondary lamellae, while endotherm III is related to the melting of lamellae, which formed through reorganization or thickening of primary and/or secondary lamellae upon heating.

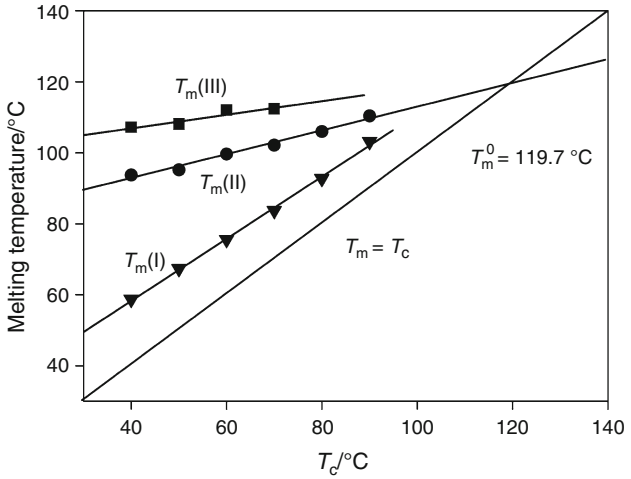

Fig. 2 Melting temperatures of isothermally melt-crystallized PHBHHx as a function of T_c

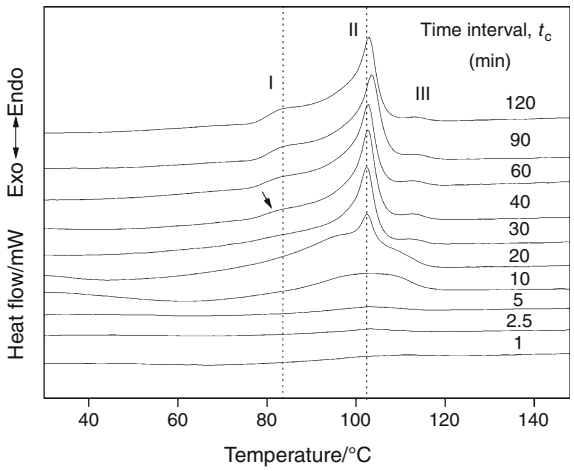

Fig. 3 Subsequent melting curves of PHBHHx samples after partial isothermal melt-crystallization at 70 °C for different time intervals as indicated

It is well known that the perfection of the crystals is determined by the T_c under isothermal conditions. As expected, crystallization at low T_c occurred under large supercooling at fast rates and led to the formation of defective crystalline structures. The latter undergoes extensive recrystallization upon subsequent heating above the T_c. In contrast, crystallization at high T_c proceeded at a slower rate accompanied by a simultaneous annealing. It resulted in more uniform thickness distribution and perfect crystals, which was confirmed by the occurrence of sharper and higher melting peaks II in Fig. 1. As T_c increased, more fraction of the sample crystallized perfectly, while the fraction which would undergo recrystallization upon heating decreased. This resulted in a decrease of endotherm III (Fig. 1), indicating that the recrystallization process started right after the melting of primary and/or secondary crystals and stopped before final melting. Nevertheless, the recrystallization rate of the molten materials may be too fast to be detected by the experimental procedure used here.

The T_m of all subsequent melting PHBHHx are shown in Fig. 2. The solid lines show the results of linear fitting curves. In Fig. 2, T_m(I) shifts to high temperature with increasing T_c and occurs at ca. 10–20 °C above the crystallization or annealing temperature, and the fitting curve is almost parallel to the line $T_m = T_c$, suggesting a typical annealing peak [3, 6]. Meanwhile, T_m(II) and T_m(III) steadily increase with the increase of T_c. If endotherm II reflects the thickness of original crystalline lamellae, the equilibrium melting temperature (T_m^0) of PHBHHx is 119.7 °C determined by the Hoffman–Weeks extrapolation [44]. This is consistent with Chen's results [38] that the T_m^0 of PHBHHx (3HHx = 12 mol%) was 121.8 °C, which is lower than those of PHBHHx with 12 and 14.6% of 3HHx (140.4 and 194 °C, respectively [41, 42]).

The weakest melting endotherm A is similar to an annealing peak, and its position is almost unaffected by T_c. It appears at around 40–50 °C. This peak possibly associates with the melting of defective crystals formed during secondary crystallization at room temperature and it will be discussed later in detail.

Sequence of crystallization

In order to investigate the sequence of crystal formation during isothermal melt-crystallization process, the samples were isothermally crystallized at a given T_c for different periods of time followed by cooling to 20 °C and rapidly heating to complete melting (150 °C) at 10 °C min^{-1}. The DSC data of those samples which were melt-crystallized at 70 °C for different durations are shown in Fig. 3. As seen in Fig. 3, almost no melting endotherm was present in traces after crystallization for 1 min, demonstrating that a time interval of at least 1 min is required for the melting peak to be observed in the subsequent melting endotherm at 70 °C. With increasing crystallization time from 2.5 to 5 min, endotherm II appeared firstly indicating that an apparent induction time is necessary for the formation of stable crystallites at the respective T_cs. After crystallization for 10 min, a broad melting endotherm, endotherm II, was found easily. Since endotherm II was observed at the onset of crystallization, it was attributed to the melting of these primary lamellae. Furthermore, it should be noted that a broad exothermic peak was also observed at low temperature region in this trace probably due to the occurrence of supplementary cold-crystallization during heating process.

As demostrated in Fig. 3, endotherm I can be seen with a careful inspection when time interval t_c = 40 min (indicated by an arrow). It suggested that the minor endotherm

associating with a rather slow crystallization process at T_c perhaps resulted from the secondary crystallization. After crystallization for 40 min, all the other three endotherms (I, II, and III) appeared. It is somewhat different from observations reported by Hu et al. [41] that endotherms II and III appeared simultaneously when $t_c = 10$ min, and endotherm I had not been observed until $t_c = 40$ min. Based on the observation above, we can conclude that an unstable lamella was unlikely produced at the beginning of the crystallization, but started to form before primary crystallization stopped. Clearly, they are related to the onset of the secondary process and the secondary nucleation occurred even at relatively low crystallinity.

There are many different explanations for the origin of endotherm I. Chen et al. [38] suggested that the annealing peak originated from the pre-melting behavior of PHBHHx in their isothermal crystallization experiment, which corresponded to an intermediate state between ordered crystalline and amorphous states [43]. However, the pre-melting behavior was not observed in the DSC curves of non-isothermal crystallization [38, 39]. In our view, this can be explained by the fact that the secondary crystallization cannot happen at all during the non-isothermal crystallization at the cooling rates used in the literature. This process is much slower than the primary crystallization and needs a relatively long period of time, that is, at least 40 min in this study.

Effect of heating rate

Heating rate effect is a common measurement to test whether the melting–recrystallization–remelting phenomena exists in semicrystalline polymers [29, 34, 35, 41] during heating. Based on the melting–recrystallization–remelting mechanism, the magnitudes of endotherm A, I, and II were expected to increase and their melting peaks shifted to higher temperatures, while the magnitude of endotherm III decreased and T_m(III) shifted to a lower temperature with the increase of heating rate.

DSC measurements (Fig. 4) at different heating rates were performed on PHBHHx sample which was isothermally crystallized at 70 °C for 24 h. The results clearly indicated that endotherms A and I increase in magnitude and shift to higher temperature with increasing heating rate. Endotherm II shifted slightly to higher temperature too. The increase in three endotherms is probably a result of superheating effect. In comparison, endotherm III gradually decreased and disappeared at a heating rate of 20 °C min^{-1} and above. Furthermore, consistent with what has been reported in literatures [29, 34, 41], endotherm I merged with endotherm II at high heating rates, indicating the existence of a recrystallization process at high temperature during heating.

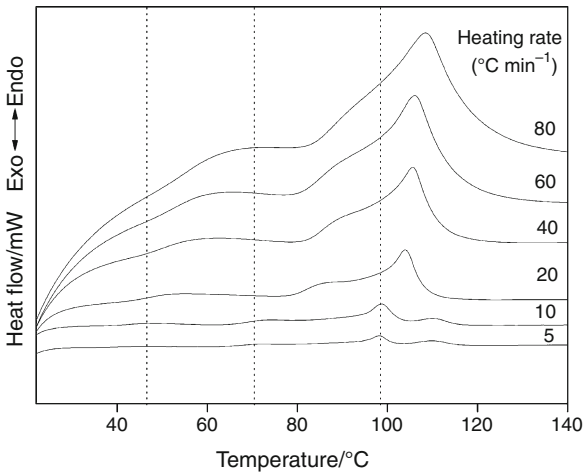

Fig. 4 Subsequent melting curves of PHBHHx samples at different heating rates after isothermal melt-crystallization at 70 °C for 24 h

It is known that some semicrystalline polymers crystallized as metastable lamellae, and which is also the reason why recrystallization or reorganization is possible during a DSC heating scan. The metastable lamellae have lowered their melting temperatures owing to their large surface/volume ratios and the high surface-free energies of their fold surfaces. At low heating rates, the time is enough for the initially existing crystals to melt and form thicker and more stable lamellae during the heating scan. However, at higher heating rates, initially existing crystals melt but recrystallization cannot occur due to the limited residence time at T_c. Moreover, the extent of recrystallization process depends on the scanning rate used. The higher the heating rate used, the shorter the time being available for the diffusion of the molecular segments onto growth front of the recrystallizing lamellae. Therefore, in terms of melting–recrystallization–remelting processes during heating, an increase in heating rate leads to a shift of the high endotherm to a lower temperature as well as a decrease in its magnitude.

Secondary crystallization at room temperature

The appearance of the endotherm A is an interesting phenomenon. As illustrated in Fig. 1, minor endothermic peaks were observed at 40–50 °C in the low temperature region. To probe the origin of these minor melting peaks, it is necessary to investigate how the minor endotherms change as the annealing time increased. The secondary crystallization is known to be a very slow process and often lags behind the primary crystallization. From the results mentioned above, we have learned that the endotherm I (secondary crystallization at $T_c = 70$ °C) did not appear until $t_c = 40$ min. Figure 5 shows the subsequent melting curves of PHBHHx samples which were isothermally

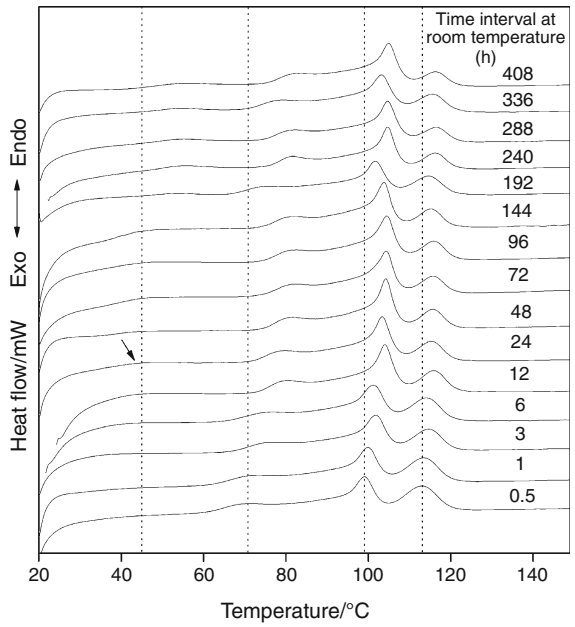

Fig. 5 Subsequent melting curves of PHBHHx samples isothermally melt-crystallized at 70 °C for 1 day and stored at room temperature for different times (heating rate 10 °C min^{-1})

crystallized from the melt at 70 °C for 1 day and stored at room temperature for different times. Clearly, after melt-crystallization at 70 °C for 1 day without storage at room temperature, no endotherm A was found. Therefore, it is reasonable to postulate that this minor endotherm may arise from the storage at room temperature (~20 °C).

However, the viscosity of crystallized material is higher at low T_c than that at high T_c, which makes the structural adjustment and diffusion of polymer chains more difficult to some extent. This also means that the secondary crystallization at room temperature (~20 °C) may require longer time to occur. As shown in Fig. 5, when the time interval at room temperature was 0.5–12 h, no endotherm was observed at 40–50 °C. Until the time interval reached 24 h, a minor endotherm (indicated by an arrow) emerged at the same position. Combining with previous DSC results, it is reasonable to conclude that this endotherm was possibly because of the melting of some crystals formed during the long-time annealing at room temperature. Moreover, as shown in Fig. 1, the endotherm A was very weak at $T_c = 40$ °C, and became an apparent peak (44–47 °C) at $T_c = 50$, 60, and 70 °C, but the peak melting temperature of endotherm A shifted toward higher temperature slightly (47–52 °C) at $T_c = 80$ and 90 °C, especially at 80 °C. Therefore, it is important to point out that the process of secondary crystallization at room temperature is heterogeneous, which depends not only on the presence of primary lamellae, but also the existence of earlier formed secondary lamellae.

Conclusions

The multiple melting behavior of isothermally melt-crystallized PHBHHx was studied by DSC analysis. Fourfold endothermic peaks were observed during the subsequent heating scan, which were named as A, I, II, and III from low to high temperature, respectively. The origin of the multiple melting temperatures phenomenon was discussed. Endotherm A was associated with the melting of secondary lamellae formed at room temperature, endotherm I corresponded to the melting of secondary crystallization at crystallization temperature, endotherm II was a result of the melting of primary lamellae, and endotherm III was related to the melting of the lamellae, which have been formed through reorganization or thickening upon heating. Furthermore, the crystallizability of copolymer depends strongly on the sequence length of the crystallizable comonomer units. Therefore, the sequence structure (configuration), sequence length, and sequence-length distribution should be characterized by, for examples, NMR, MS, and SAXS. More work should be conducted in the future to verify this proposal.

Acknowledgements The authors gratefully acknowledge the financial support of this work by the Tianjin Municipal Natural Science Foundation of China (Contract grant number: 08JCZDJC24600). We also thank Prof. S. Z. Wu for his work on the differential scanning calorimetry and helpful discussions.

References

1. Sudesh K, Abe H, Doi Y. Synthesis, structure and properties of polyhydroxyalkanoates: biological polyesters. Prog Polym Sci. 2000;25:1503–55.
2. Chen GQ, Wu Q. The application of polyhydroxyalkanoates as tissue engineering materials. Biomaterials. 2005;26:6565–78.
3. Lenz RW, Marchessault RH. Bacterial polyesters: biosynthesis, biodegradable plastics and biotechnology. Biomacromolecules. 2005;6:1–8.
4. Doi Y, Kitamura S, Abe H. Microbial synthesis and characterization of poly(3-hydroxybutyrate-co-3-hydroxyhexanoate). Macromolecules. 1995;28:4822–8.
5. Asrar J, Valentin HE, Berger PA, Tran M, Padgette SR, Garbow JR. Biosynthesis and properties of poly(3-hydroxybutyrate-co-3-hydroxyhexanoate) polymers. Biomacromolecules. 2002;3:1006–12.
6. Fukui T, Abe H, Doi Y. Engineering of ralstonia eutropha for production of poly(3-hydroxybutyrate-co-3-hydroxyhexanoate) from fructose and solid-state properties of the copolymer. Biomacromolecules. 2002;3:618–24.
7. Qiu YZ, Ouyang SP, Shen ZY, Wu Q, Chen GQ. Metabolic engineering for the production of copolyesters consisting of 3-hydroxybutyrate and 3-hydroxyhexanoate by *Aeromonas hydrophila*. Macromol Biosci. 2004;4:255–61.
8. Chen GQ, Zhang G, Park SJ, Lee SY. Industrial scale production of poly(3-hydroxybutyrateco-3-hydroxyhexanoate). Appl Microbiol Biotechnol. 2001;57:50–5.
9. Deng Y, Zhao K, Zhang XF, Hu P, Chen GQ. Study on the three-dimensional proliferation of rabbit articular cartilage-derived

chondrocytes on polyhydroxyalkanoate scaffolds. Biomaterials. 2002;23:4049–56.
10. Deng Y, Lin XS, Zheng Z, Deng JG, Chen JC, Ma H, Chen GQ. Poly(hydroxybutyrate-co-hydroxyhexanoate) promoted production of extracellular matrix of articular cartilage chondrocytes in vitro. Biomaterials. 2003;24:4273–81.
11. Zhao K, Deng Y, Chen JC, Chen GQ. Polyhydroxyalkanoate (PHA) scaffolds with good mechanical properties and biocompatibility. Biomaterials. 2003;24:1041–5.
12. Wang Y, Bian YZ, Wu Q, Chen GQ. Evaluation of three-dimensional scaffolds prepared from poly(3-hydroxybutyrate-co-3-hydroxyhexanoate) for growth of allogeneic chondrocytes for cartilage repair in rabbits. Biomaterials. 2008;29:2858–68.
13. Zhao K, Yang X, Chen GQ, Chen JC. Effect of lipase treatment on the biocompatibility of microbial polyhydroxyalkanoates. J Mater Sci. 2002;13:849–54.
14. Yang XS, Zhao K, Chen GQ. Effect of surface treatment on the biocompatibility of microbial polyhydroxyalkanoates. Biomaterials. 2002;23:1391–7.
15. Wang YW, Yang F, Wu Q, Cheng YC, Yu PHF, Chen JC, Chen GQ. Effect of composition of poly(3-hydroxybutyrate-co-3-hydroxyhexanoate) on growth of fibroblast and osteoblast. Biomaterials. 2005;26:755–61.
16. Wang YW, Wu Q, Chen GQ. Attachment, proliferation and differentiation of osteoblasts on random biopolyester poly(3-hydroxybutyrate-co-3-hydroxyhexanoate) scaffolds. Biomaterials. 2004;25:669–75.
17. Qu XH, Wu Q, Liang J, Qu X, Wang SG, Chen GQ. Enhanced vascular-related cellular affinity on surface modified copolyesters of 3-hydroxybutyrate and 3-hydroxyhexanoate (PHBHHx). Biomaterials. 2005;26:6991–7001.
18. Qu XH, Wu Q, Liang J, Zou B, Chen GQ. Effect of 3-hydroxyhexanoate content in poly(3-hydroxybutyrate-co-3-hydroxyhexanoate) on in vitro growth and differentiation of smooth muscle cells. Biomaterials. 2006;27:2944–50.
19. Chen S, Wang PP, Wang JP, Chen GQ, Wu Q. Guided growth of smooth muscle cell on poly(3-hydroxybutyrate-co-3-hydroxyhexanoate) scaffolds with uniaxial microtubular structures. J Biomed Mater Res A. 2008;86:849–56.
20. Bian YZ, Wang Y, Aibaidoula G, Chen GQ, Wu Q. Evaluation of poly(3-hydroxybutyrate-co-3-hydroxyhexanoate) conduits for peripheral nerve regeneration. Biomaterials. 2009;30:217–25.
21. Ahmed J, Zhang JX, Song Z, Varshney SK. Thermal properties of polylactides Effect of molecular mass and nature of lactide isomer. J Therm Anal Calorim. 2009;95:957–64.
22. Souza JDL, Kobelnik M, Ribeiro CA, Capela JMV, Crespi MS. Kinetic study of crystallization of PHB in presence of hydroxy acids. J Therm Anal Calorim. 2009;97:525–8.
23. Mothé CG, Azevedo AD, Drumond WS, Wang SH. Thermal properties of amphiphilic biodegradable triblock copolymer of L,L-lactide and ethylene glycol. J Therm Anal Calorim. 2010;101:229–33.
24. Nunes PS, Bezerra MS, Costa LP, Cardoso JC, Albuquerque RLC Jr, Rodrigues MO, Barin GB, Silva FAD, Araújo AAS. Thermal characterization of usnic acid/collagen-based films. J Therm Anal Calorim. 2010;99:1011–4.
25. Yoo ES, Im SS. Melting behavior of poly(butylene succinate) during heating scan by DSC. J Polym Sci B Polym Phys. 1999;37:1357–66.
26. Yasuniwa M, Satou T. Multiple melting behavior of poly(butylene succinate) I. Thermal analysis of melt-crystallized samples. J Polym Sci B Polym Phys. 2002;40:2411–20.
27. Qiu ZB, Komura M, Ikehara T, Nishi T. DSC and TMDSC study of melting behaviour of poly(butylene succinate) and poly(ethylene succinate). Polymer. 2003;44:7781–5.
28. Yasuniwa M, Tsubakihara S, Satou T, Iura K. Multiple melting behavior of poly(butylene succinate) II. thermal analysis of isothermal crystallization and melting process. J Polym Sci B Polym Phys. 2005;43:2039–47.
29. Ling XY, Spruiell JE. Analysis of the complex thermal behavior of poly(L-lactic acid) film. I. samples crystallized from the glassy state. J Polym Sci B Polym Phys. 2006;44:3200–14.
30. Pan PJ, Kai WH, Zhu B, Dong T, Inoue Y. Polymorphous crystallization and multiple melting behavior of poly(L-lactide): molecular weight dependence. Macromolecules. 2007;40:6898–905.
31. Gunaratne LMWK, Shanks RA, Amarasinghe G. Thermal history effects on crystallisation and melting of poly(3-hydroxybutyrate). Thermochim Acta. 2004;423:127–35.
32. Gunaratne LMWK, Shanks RA. Multiple melting behaviour of poly(3-hydroxybutyrate-co-hydroxyvalerate) using step-scan DSC. Euro Polym J. 2005;41:2980–8.
33. Gunaratne LMWK, Shanks RA. Melting and thermal history of poly(hydroxybutyrate-co-hydroxyvalerate) using step-scan DSC. Thermochim Acta. 2005;430:183–90.
34. Liu T, Petermann J. Multiple melting behaviour in isothermally cold-crystallized isotactic polystyrene. Polymer. 2001;42:6453–61.
35. Watanabe T, He Y, Fukuchi T, Inoue Y. Comonomer compositional distribution and thermal characteristics of bacterially synthesized poly(3-hydroxybutyrate-co-3-hydroxyhexanoate)s. Macromol Biosci. 2001;1:75–83.
36. Abe H, Doi Y, Aoki H, Akehata T. Solid-state structures and enzymatic degradabilities for melt-crystallized films of copolymers of (R)-3-hydroxybutyric acid with different hydroxyalkanoic acids. Macromolecules. 1998;31:1791–7.
37. Feng L, Watanabe T, Wang Y, Kichise T, Fukuchi T, Chen GQ, Doi Y, Inoue Y. Studies on comonomer compositional distribution of bacterial poly(3-hydroxybutyrate-co-3-hydroxyhexanoate)s and thermal characteristics of their factions. Biomacromolecules. 2002;3:1071–7.
38. Chen C, Cheung MK, Yu PHF. Crystallization kinetics and melting behaviour of microbial poly(3-hydroxybutyrate-co-3-hydroxyhexanoate). Polym Int. 2005;54:1055–64.
39. Sato H, Nakamura M, Padermshoke A, Yamaguchi H, Terauchi H, Ekgasit S, Noda I, Ozaki Y. Thermal behavior and molecular interaction of poly(3-hydroxybutyrate-co-3-hydroxyhexanoate) studied by Wide-angle X-ray diffraction. Macromolecules. 2004;37:3763–9.
40. Feng L, Watanabe T, He Y, Wang Y, Kichise T, Fukuchi T, Chen GQ, Doi Y, Inoue Y. Phase behavior and thermal properties for binary blends of bacterial poly(3-hydroxybutyrate-co-3-hydroxyhexanoate)s with narrow-comonomer-unit compositional distribution. Macromol Biosci. 2003;3:310–9.
41. Hu Y, Zhang JM, Sato H, Noda I, Ozaki Y. Multiple melting behavior of poly(3-hydroxybutyrate-co-3-hydroxyhexanoate) investigated by differential scanning calorimetry and infrared spectroscopy. Polymer. 2007;48:4777–85.
42. Gan ZH, Kuwabara K, Abe H, Doi Y. The solid-state structure, thermal and crystalline properties of bacterial copolyesters of (R)-3-hydroxybutyric acid with (R)-3-hydroxyhexanoic acid. Biodegradable polymers and plastics. In: Proceedings of the seventh world conference on biodegradable polymers & plastics, Terrenia, Italy, June 4–8, 2002 (2003), Meeting Date 2002, p. 167–184.
43. Wu Q, Tian G, Sun SQ, Noda I, Chen GQ. Study of microbial polyhydroxyalkanoates using two-dimensional Fourier-transform infrared correlation spectroscopy. J Appl Polym Sci. 2001;82:934–40.
44. Hoffman JD, Weeks JJ. Melting process and the equilibrium melting temperature of polychlorotrifluoroethylene. J Res Natl Bur Stand. 1962;A66:13–28.